1997

Heat-Treatment Behavior of High-Palladium Dental Alloys

Qiang Wu
The Ohio State University

William A. Brantley
The Ohio State University

John C. Mitchell
The Ohio State University

Stanley G. Vermilyea
The Ohio State University

Jianzhong Xiao
The Chinese University of Hong Kong

See next page for additional authors

Utah State University
MERRILL-CAZIER LIBRARY

Heat-Treatment Behavior of High-Palladium Dental Alloys

Authors

Qiang Wu, William A. Brantley, John C. Mitchell, Stanley G. Vermilyea, Jianzhong Xiao, and Wenhua Guo

HEAT-TREATMENT BEHAVIOR OF HIGH-PALLADIUM DENTAL ALLOYS

Qiang Wu, William A. Brantley[*], John C. Mitchell[1], Stanley G. Vermilyea, Jianzhong Xiao[2], and Wenhua Guo[2]

College of Dentistry, and [1]Department of Geological Sciences, The Ohio State University, Columbus, Ohio 43210
[2]Department of Physics, The Chinese University of Hong Kong, Shatin, New Territories, Hong Kong

Abstract

Four high-palladium dental alloys were cast, quenched following solidification, and heat treated at temperatures ranging from 200° to 1,800°F. The Vickers hardness of each alloy was measured, and microstructural changes were studied by scanning electron microscopy (SEM). Phase transformations were investigated by thermomechanical analysis (TMA). Heat treatment at 1,600° and 1,800°F significantly decreased the hardness of one Pd-Cu-Ga alloy, compared to the as-cast condition, as did heat treatment at 1,800°F for the other Pd-Cu-Ga alloy and one Pd-Ga alloy, and yielded fine-grained microstructures of the palladium solid solution. There were generally no significant changes in the hardness of the other Pd-Ga alloy for heat treatments over the entire temperature range, which was attributed to persistence of the as-cast dendritic structure. For all alloys, heat treatment at 1,200°F resulted in formation of discontinuous precipitates, which had very similar hardness to that of the palladium solid solution. Variations in the amount of a previously unidentified hard phase with temperature were assumed to account for the hardness variations in the harder Pd-Cu-Ga alloy. The TMA results suggested that a second-order phase transformation occurred around 1,050° to 1,400°F in all alloys, which may be formation of an ordered tweed structure observed by transmission electron microscopy in another study.

Key Words: Palladium, dental alloy, heat treatment, microstructure, discontinuous precipitate, eutectic, scanning electron microscopy, microhardness, thermomechanical analysis.

[*]Address for correspondence:
William A. Brantley
Sec. Restorat. Dentistry, Prosthodontics & Endodontics
College of Dentistry, The Ohio State University
305 West 12th Avenue, Columbus, Ohio 43210-1241
Telephone number: (614) 292-0773
FAX number: (614) 292-9422
E-mail: brantley.1@osu.edu
or E-mail: wbrantle@columbus.rr.com

Introduction

The high-palladium dental alloys contain more than 75 wt.% palladium and are derived from the Pd-Cu-Ga or Pd-Ga systems, with small amounts of other elements such as gold, silver, tin, indium and cobalt (Brantley et al., 1993). The high-palladium alloys have lower unit metal cost compared to gold alloys, good mechanical properties and no problems with porcelain discoloration (Carr and Brantley, 1991). The Pd-Cu-Ga dental alloys containing approximately 10 wt.% copper and 6-9 wt.% gallium date from the patent by Schaffer (1983) for the Option alloy (J.M. Ney Company, Bloomfield, CT), and have much higher hardness and yield strength than the subsequently introduced copper-free alloys based on the Pd-Ga system. There may be some concern (Carr and Brantley, 1991) that the hardness of Pd-Cu-Ga alloys often exceeds that for tooth enamel where the Knoop hardness is approximately 340 (Craig, 1993), but the high yield strength of these alloys is offset by their lower elastic modulus compared to base metal and noble metal dental alloys (Bertolotti, 1997). Asgar (1988) has stated that the high-palladium alloys are the noble metals of the future in dentistry, because of their excellent properties and lower unit metal cost than the gold alloys. The high-palladium alloys have also become important for implant-supported prostheses because of their relatively high values of strength and ductility (Stewart et al., 1992).

The metallurgical starting point for the high-palladium alloys is the Pd-Ga phase diagram. The revised version of this phase diagram (Fig. 1), which has been published by the American Society for Metals (Massalski, 1990), is based upon research by Khalaff and Schubert (1974). There have been considerable changes in the high-Pd end of this diagram, compared to the previous version published by the American Society for Metals (Massalski, 1986), which was based upon much earlier research by Schubert et al. (1959). The peritectoid reaction at approximately 1,560°F on cooling (Pd$_2$Ga + Pd solid solution → Pd$_3$Ga) is no longer shown on the Pd-Ga phase diagram (Massalski, 1990). Instead, Pd$_2$Ga is indicated as congruently melting, stable to room temperature, and with a single-phase field

Atomic Percent Palladium
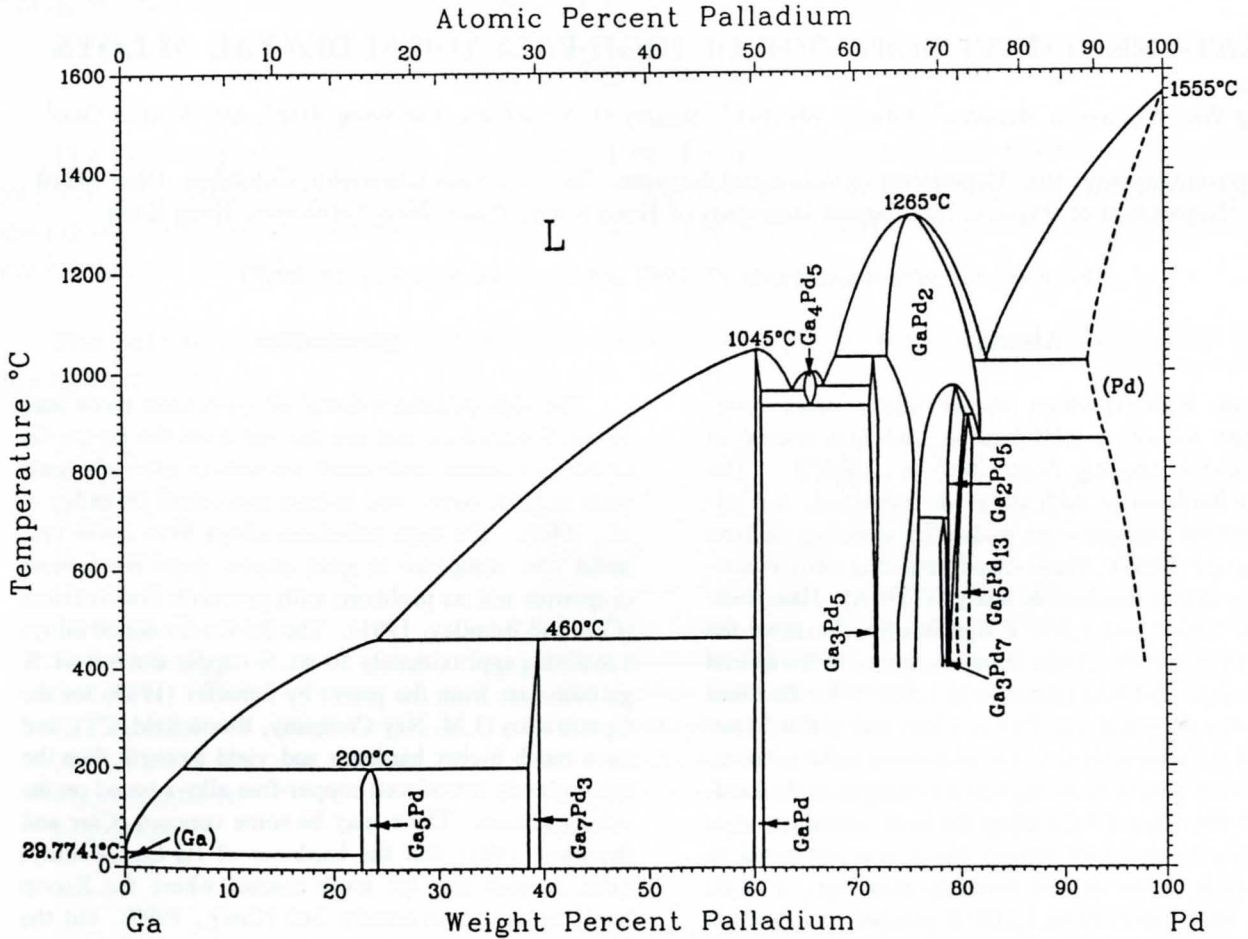
Figure 1. Current version of the Pd-Ga phase diagram (Massalski, 1990). (Reproduced by permission of ASM International).

---

extending to over 80 wt. % Pd at 1,800°F. Three new phases exist over a relatively narrow composition range: Pd_5Ga_2 forms directly from Pd_2Ga, whereas Pd_7Ga_3 and $Pd_{13}Ga_5$ form by peritectoid reactions on cooling.

Because the high-palladium alloys contain several other elements besides palladium, numerous phases would be expected in their microstructures under equilibrium conditions (Darken and Gurry, 1953). However, these alloys experience relatively rapid solidification under normal dental casting conditions (Phillips, 1991), and non-equilibrium microstructures and microsegregation occur. Although subsequent heat treatment simulating the dental porcelain firing cycles causes microstructural changes in representative as-cast high-palladium alloys, large changes in Vickers hardness and presumably yield strength (Dieter, 1986) are not observed (Brantley *et al.*, 1993; Carr *et al.*, 1993).

At present, only limited scientific information is available about the metallurgical structure of high-palla-

dium alloys. Khabliyev *et al.* (1980) used X-ray diffraction (XRD) to investigate the heat-treatment response of a non-dental Pd-Cu-Ga alloy. Using transmission electron microscopy (TEM), Odén and Herø (1986) concluded that a complex submicron network of face-centered tetragonal (fct) $Pd_3Ga_xCu_{1-x}$ precipitates was responsible for the high hardness and strength of a commercial 79Pd-10Cu-9Ga-2Au dental alloy. They further suggested that the absence of this precipitate network in an experimental Pd-Cu-Ga alloy of different composition accounted for its lower strength and hardness. Mezger *et al.* (1988) subsequently used XRD to study the metallurgical structure of numerous commercial Pd-Cu-Ga dental alloys in the as-cast condition and after simulated porcelain firing heat treatment. While these investigators reported the presence of secondary phases, in addition to the palladium solid solution matrix, they were generally unable to identify the other phases. Brantley *et al.* (1995) similarly found that the limited amounts of

Table 1. Nominal compositions (wt. %) of the four high-palladium alloys studied, as provided by the manufacturers.

Alloy	Palladium	Copper	Gallium	Indium	Tin	Gold	Silver
Liberty[‡,*]	76	10	5.5	—	6	2	—
Freedom Plus[‡,*]	78	8	5	6	—	2	—
Legacy XT[‡,*]	75.5	—	6	6	—	2	10
IS 85[†]	82	—	6	3.5	3.5	2.5	2.5

[*]These alloys also contain small amounts of ruthenium as a grain-refining element.

[†]Williams Dental Co., Div. Ivoclar No. America, Amherst, NY.　　　　　[‡]J.F. Jelenko & Co., Armonk, NY.

Table 2. Properties[*] of the four high-palladium alloys, as provided by the manufacturers.

Alloy	Yield Strength (MPa)	Vickers Hardness	Elastic Modulus (GPa)	Percentage Elongation (%)	Melting Range (°F)
Liberty	724	340	145	15	2,010-2,280
Freedom Plus	566	265	138	30	2,140-2,370
Legacy XT	550	245	128	30	2,175-2,370
IS 85	445	240	141	41	2,130-2,435
	466	260	141	37	

[*]For IS 85 the 0.1% offset yield strength is provided. The upper values of the mechanical properties correspond to the alloy after porcelain firing, whereas the lower values are after the hardening heat treatment. For Liberty, Freedom Plus and Legacy XT, 0.2% offset yield strength values are provided, and mechanical properties are for the alloys after porcelain firing.

secondary microstructural phases failed to yield significant peaks in the XRD patterns for representative as-cast commercial Pd-Ga alloys.

In the written discussion to a previous article (Brantley et al., 1993), Dr. H.J. Mueller noted that it might be worthwhile to perform post-casting heat treatments for high-palladium dental alloys to modify the mechanical properties as needed for various clinical applications, such as metal-ceramic restorations, implant-supported prostheses, and perhaps all-metal restorations or partial denture frameworks. Because of uncertainties in the Pd-Ga phase diagram (Massalski, 1986, 1990) that provides the foundation for the high-palladium dental alloys, the lack of equilibrium conditions during dental casting, and the typically brief porcelain firing cycles (Papazoglou et al., 1993), it has not been possible to establish precise mechanisms about the microstructural changes following simulated porcelain-firing heat treatment. Moreover, since the temperature is rapidly varied from approximately 1,000° to 1,800° F during the por-

celain firing cycles, it has not been possible in previous research (Brantley et al., 1993; Carr et al., 1993) to determine the effects of specific heat-treatment temperatures on the Vickers hardness of high-palladium alloys.

The goal of the present study was to obtain detailed experimental information about the changes in Vickers hardness of four representative high-palladium alloys over the heat-treatment temperature range from 200° to 1,800°F, in order to determine whether annealing heat treatments at specific temperatures might yield significant changes in mechanical properties. Such information may permit use of these alloys with their optimum structure and properties for the treatment of dental patients.

Materials and Methods

Two Pd-Cu-Ga alloys (Freedom Plus and Liberty; J.F. Jelenko and Company, Armonk, NY) and two Pd-Ga alloys (IS 85, Williams Dental Company, Division of Ivoclar North America, Amherst, NY; Legacy XT, J.F.

Table 3. Vickers hardness of the four high-palladium alloys for different solidification conditions and heat-treatment temperatures.[*]

Condition	Liberty		Freedom Plus		Legacy XT		IS 85	
ACBC	326.0 ± 8.6	ABC	266.1 ± 7.2	A	260.1 ± 8.5	B	250.9 ± 9.0	ABC
ACRQ	318.1 ± 2.2	BCD	266.0 ± 10.6	A	280.2 ± 12.4	A	256.5 ± 11.4	ABC
200°F	309.8 ± 10.6	CD	260.3 ± 8.7	ABC	253.5 ± 7.7	B	241.7 ± 8.3	BC
400°F	322.4 ± 10.4	ABC	253.0 ± 4.5	ABC	256.9 ± 6.9	B	247.5 ± 8.2	ABC
600°F	330.8 ± 11.8	ABC	253.8 ± 3.6	ABC	257.3 ± 5.1	B	250.7 ± 9.5	ABC
800°F	333.5 ± 15.4	ABC	249.1 ± 5.9	BC	251.9 ± 5.1	B	237.0 ± 8.8	C
1,000°F	350.5 ± 20.0	A	259.2 ± 5.9	ABC	254.7 ± 7.4	B	255.0 ± 7.3	ABC
1,200°F	343.4 ± 12.2	AB	260.1 ± 10.6	ABC	262.0 ± 4.4	B	259.1 ± 4.9	AB
1,400°F	309.5 ± 11.1	CD	251.4 ± 9.9	ABC	258.7 ± 5.7	B	256.0 ± 6.9	ABC
1,600°F	289.7 ± 8.3	DE	262.2 ± 9.7	AB	249.8 ± 6.6	B	267.1 ± 8.8	A
1,800°F	267.1 ± 5.0	E	245.5 ± 5.7	C	236.6 ± 6.3	C	258.0 ± 7.6	AB

[*]For each alloy, mean values (N = 10) with the same letter were not significantly different, using the REGW test (α = 0.05). The as-cast conditions were bench cooled (ACBC) or rapidly quenched (ACRQ). Heat treatments were performed on ACRQ specimens.

Jelenko and Company) were selected for study. The alloy compositions are listed in Table 1, and some important properties are given in Table 2. The Liberty, Freedom Plus and Legacy XT alloys contain the grain-refining element ruthenium (Brantley *et al.*, 1993) and have equiaxed fine-grained as-cast microstructures, whereas IS 85 does not contain a grain-refining element and has a dendritic as-cast microstructure.

The alloys were centrifugally cast as 3 mm diameter rods, using standard dental laboratory techniques (Carr and Brantley, 1991). Wax patterns of this diameter and 20 mm length were sprued and invested in fine-grained, carbon-free, phosphate-bonded investment (Cera-Fina, Whip Mix Corp., Louisville, KY). Investment manipulation and burnout procedures followed the recommendations of the manufacturers, and a dwell time of 30 minutes at the peak burnout temperature of 1,400°F was used. Three wax patterns for each alloy were invested in one casting ring to prepare the quenched specimens, and a single wax pattern was invested in a separate ring for the bench-cooled specimen. The alloys were melted in individual ceramic crucibles and cast using a standard broken-arm casting machine (Kerr Division, Sybron Corp., Romulus, MI), as previously described (Carr and Brantley, 1991). The castings were either rapidly quenched in an ice-water mixture or bench cooled to room temperature.

After devesting (without subsequent air abrasion), the cast rods were sectioned into 3 mm diameter x 2-3 mm thick specimens, using a low-speed, water-cooled, diamond-coated saw (Vari/Cut VC-50, Leco Corp., St. Joseph, MI). Quenched specimens were subjected to 10 minute periods of heat treatment in a dental furnace (Mark IV Digital, J.M. Ney Co.) at temperatures of 200°, 400°, 600°, 800°, 1,000°, 1,200°, 1,400°, 1,600° and 1,800°F, following by quenching in ice-water again. Two specimens were used for each heat-treatment temperature.

Specimens were mounted in transparent metallographic epoxy resin (Leco Corp.), subjected to metallographic wet grinding with 400 and 600 grit silicon carbide paper, and polished using gamma alumina slurries with particle sizes of 5, 1, 0.3 and 0.05 μm. The polished specimens were etched in aqua regia solutions (Mezger *et al.*, 1988) for time periods that varied with each alloy to yield the optimum microstructure and then ultrasonically cleaned in distilled water. The Vickers hardness of each alloy was measured for the as-cast bench-cooled (ACBC), as-cast and rapidly quenched (ACRQ) and heat-treated conditions. Ten indentations were randomly located on two samples using a 1 kg load and 30 second dwell time (M-400 hardness tester, Leco Corp.). The hardness values of each alloy were compared for the different conditions using one-way analysis

of variance (ANOVA), followed by the Ryan-Einot-Gabriel-Welsch (REGW) multiple range test. In addition, a light indentation load of 10 gm that yielded Vickers indentations with diagonal lengths less than 10 μm was used to measure the hardness of individual microstructural phases or constituents for comparison with the hardness of the overall alloy.

The polished and etched specimens were first examined by a light microscope (Olympus PME, Tokyo, Japan) to assure that optimum etching was achieved. The resin-mounted specimens were then vacuum sputter-coated with a gold-palladium layer for observation with the scanning electron microscope (SEM) (JSM-820, JEOL Ltd., Tokyo, Japan). Photomicrographs of representative microstructures were made at various magnifications, using the secondary electron image (SEI) mode. Some specimens were also polished and etched again, and then coated with a carbon film for observation in the backscattered electron image (BEI) mode. Quantitative elemental composition information for selected microstructural phases was provided by X-ray energy-dispersive spectroscopic analyses (EDS), using a Link eXL microanalysis system with a PentaFET detector and an ultra-thin window (Oxford Instruments Group, High Wycombe, U.K.) coupled to the SEM. Spot analyses were performed on five different sites of carbon-coated specimens for each phase of interest.

The thermal expansion characteristics of the four high-palladium alloys from room temperature to 1,800°F were measured by a thermomechanical analysis (TMA) instrument (TMA7, Perkin-Elmer Corp., Norwalk, CT). Five specimens of each alloy were used for the TMA experiments, whose purpose was to provide complementary information about the possible occurrence of phase transformations during the heat treatment. The two ends of the 3 mm diameter disk specimens of the alloys were polished through 0.05 μm alumina slurries and lightly etched in aqua regia solutions to maintain a flat and stress-free condition. The TMA measurements were performed at 9°F per minute from 25° to 1,832°F for both the heating and cooling cycles. Argon at 30 psi served as a protection gas to prevent alloy oxidation at elevated temperatures, and the TMA probe pressure on the specimen was approximately 0.5 N.

Results and Discussion

Microhardness measurements

The mean values and standard deviations of Vickers hardness for the four high-palladium alloys with different solidification and heat-treatment conditions are listed in Table 3. For each alloy, there was an overall significant difference when all of the different conditions were compared by one-way ANOVA ($P < 0.05$). Using the REGW multiple range test, mean values for each alloy
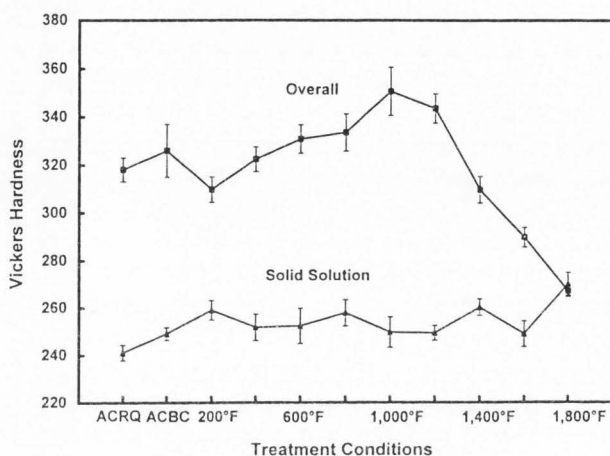
Figure 2. Vickers hardness of the overall Liberty alloy (1 kg load) and the palladium solid solution (10 g load) for two different solidification conditions (ACBC and ACRQ), and for heat treatments (ACRQ specimens) from 200°F to 1,800°F.

---

in this table with different letter codes were significantly different ($P < 0.05$). For example, there was no significant difference in hardness for as-cast specimens of the Liberty, Freedom Plus and IS 85 alloys experiencing the two solidification conditions. There was also no practical difference in the hardness of the Legacy XT alloy for the ACBC and ACRQ conditions, since differences in mean hardness of no more than 10% probably cannot be detected by dental laboratory personnel or dentists performing adjustments on castings.

Table 3 shows that the Liberty Pd-Cu-Ga alloy had the highest hardness for all conditions, while the hardness values for the other three alloys were very similar. Comparing the nominal compositions of the four alloys in Table 1, it is evident that the high copper and tin contents contributed to the greater hardness of Liberty. While the highest mean hardness for this alloy occurred after heat treatment at 1,000°F, there were no significant differences in the mean hardness for the ACBC condition and heat-treatment temperatures from 400° to 1,200°F. The lowest mean hardness occurred after heat treatment at 1,800°F, but there was no significant difference in the hardness for the heat treatments at 1,600° and 1,800°F. Use of a light load (10 g) yielding indentations within grains of the palladium solid solution (Wu, 1996) indicated that the mean hardness of this phase changed little with heat treatment and was approximately equal to the mean hardness of the overall alloy after 1,800°F heat treatment (Fig. 2).

The mean hardness values for the other Pd-Cu-Ga alloy studied, Freedom Plus, were much lower than those of Liberty. Table 1 shows that Freedom Plus

contains less copper (8 wt. %) than Liberty (10 wt. %), and 6 wt. % indium has been substituted in place of the 6 wt. % tin found in Liberty. Both tin and indium can form oxides during the porcelain firing cycles and contribute to the metal-ceramic adherence (van der Zel, 1988; Brantley *et al.*, 1996a). From Table 3, it can be seen that there were essentially no significant differences in Vickers hardness for any of the solidification and heat-treatment conditions for this alloy, other than heat treatment at 1,800°F. Even in this case, since the decrease in hardness compared to the ACBC and ACRQ conditions was less than 10%, the change would have no clinical significance. The difference in the hardness values of Liberty and Freedom Plus can be explained from the microstructures of these alloys, as discussed in the next section.

For the Pd-Ga alloy Legacy XT, there were no significant differences in hardness for any of the conditions, except for the ACRQ specimens and the heat treatment at 1,800°F (Table 3). It might be conjectured that the slight increase in hardness for the ACRQ specimens compared to the ACBC condition was associated with additional residual stress in the castings, although this effect was not observed with the other three as-cast alloys. The decrease in hardness after heat treatment at 1,800°F was attributed to dissolution of microstructural precipitates, as discussed in the next section. For the other Pd-Ga alloy IS 85, the small changes found in mean hardness for the different conditions had little statistical or practical significance. Precipitation processes may also account for these minor changes, as discussed in the next section.

Table 3 indicates that the hardness values of Freedom Plus, Legacy XT and IS 85 were very similar to that of Liberty after heat treatment at 1,800°F, whose hardness is mainly attributed to the palladium solid solution. It thus appears that microstructural precipitates have only minor contributions to the Vickers hardness (and presumably yield strength) of Freedom Plus, Legacy XT and IS 85.

Microstructural studies

The as-cast Pd-Cu-Ga alloy Liberty has a fine-grained microstructure with a near-surface lamellar eutectic constituent consisting of the palladium solid solution and Pd_2Ga (Brantley *et al.*, 1993). The photomicrograph in Figure 3 for ACRQ Liberty shows a one-grain-wide surface zone that is depleted of the eutectic constituent, as well as a zone with a high prevalence of the eutectic structure just beneath it. The microstructure of ACRQ Liberty contains more rod-shaped eutectic morphology compared to the ACBC condition (Brantley *et al.*, 1996b).

The presence of a near-surface eutectic structure in

Figures 3-8 are on the facing page 167

Figure 3. Secondary electron image of as-cast and rapidly quenched (ACRQ) Pd-Cu-Ga alloy Liberty, showing the distribution of the eutectic constituent over the specimen cross-section. Bar = 100 μm.

Figure 4. Secondary electron image of the near-surface region of ACRQ Liberty, where the hard and surrounding grain boundary phases are designated by (H) and (G), respectively. Bar = 10 μm.

Figure 5. Secondary electron image of the bulk microstructure of Liberty after heat treatment at 1,200°F, showing discontinuous precipitates (D). Areas of the hard phase (H) and surrounding phase (G) shown in Figure 4 have also been designated. Bar = 10 μm.

Figure 6. Secondary electron image of Liberty after heat treatment at 1,800°F, showing that the discontinuous precipitates have dissolved in the palladium solid solution. Some white-appearing Ru-rich precipitates (Brantley *et al.*, 1993) can be seen, and island-shaped grain-boundary Pd_2Ga precipitates have been revealed by light etching. Bar = 10 μm.

Figure 7. Secondary electron image of as-cast and bench-cooled (ACBC) Pd-Cu-Ga alloy Freedom Plus, showing a fine-grained microstructure with some areas of a grain boundary eutectic structure (E), residual interdendritic regions (I), a grain boundary phase (G) and Ru-rich precipitates (R). Bar = 10 μm.

Figure 8. Secondary electron image of Freedom Plus after heat treatment at 1,200°F, showing the formation of lamellar discontinuous precipitates. A cluster of Ru-rich precipitates can also be seen. Bar = 10 μm.

Liberty arises (Carr and Brantley, 1991; Brantley *et al.*, 1993) from the shifting of the Pd-Ga binary eutectic composition (Fig. 1) to higher palladium concentrations with the addition of copper (Cascone, 1984) and the effect of the rapid solidification conditions associated with dental casting (Phillips, 1991) on the liquidus curve (Reed-Hill and Abbaschian, 1994). During solidification, the higher-melting palladium solid solution forms first at the investment surface, leaving a Ga-rich liquid just below it that subsequently transforms to a structure containing a high percentage of eutectic. Consequently, the surface of the casting has a narrow palladium solid solution zone devoid of the eutectic structure, followed by a eutectic-rich zone. At greater distances from the surface where the cooling rate is less, only small amounts of the eutectic structure are found (Carr and Brantley, 1991).
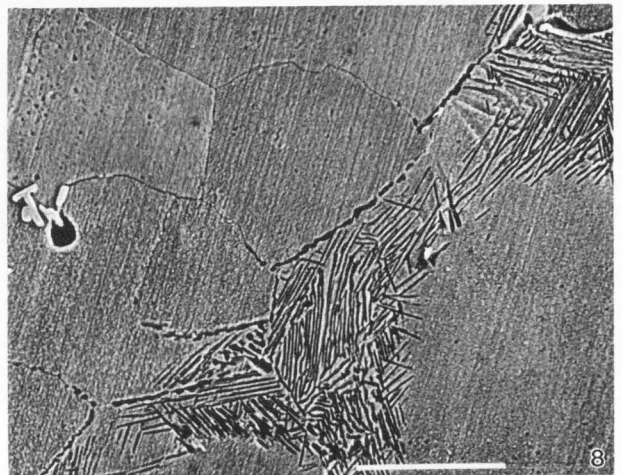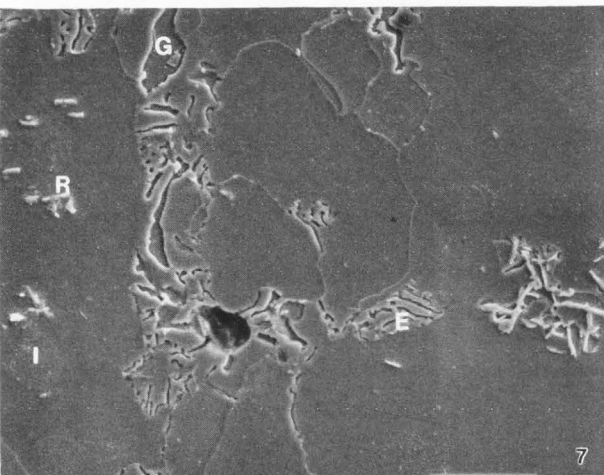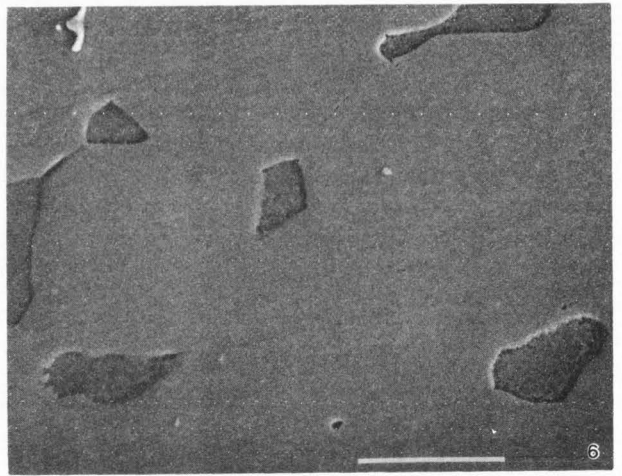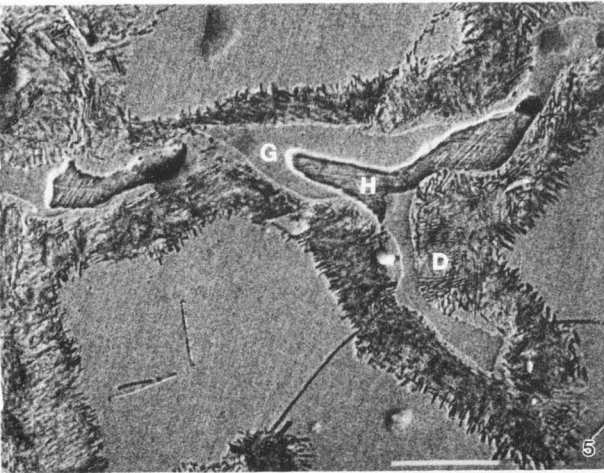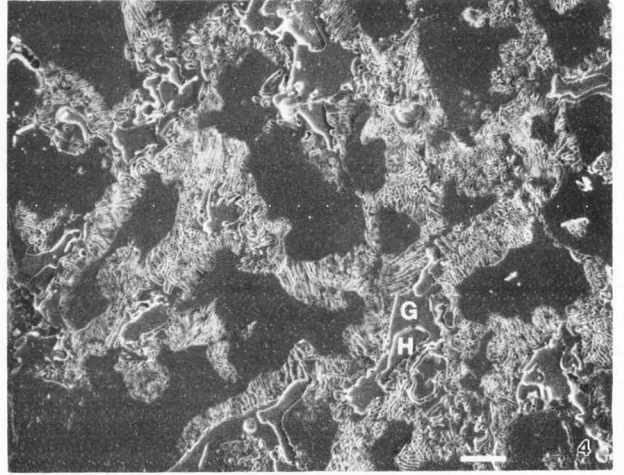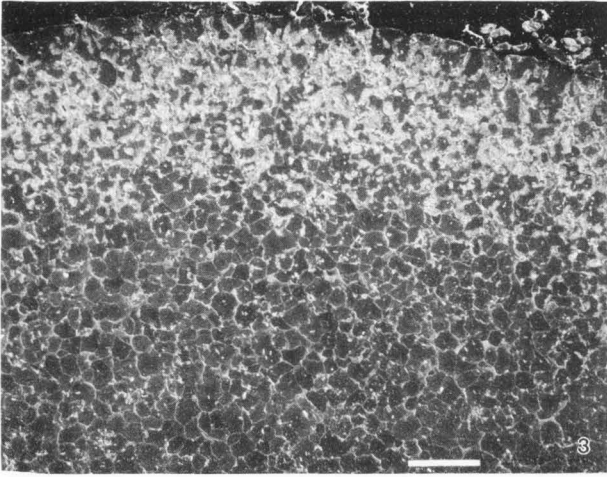
In both ACBC and ACRQ Liberty, a previously un-identified and irregular grain boundary phase, indicated by the letter (H) in Figure 4, was the hardest constituent, with a Vickers hardness exceeding 400. This phase was usually surrounded by another previously unidentified grain boundary phase (indicated by the letter G) with a hardness of approximately 350. EDS analyses indicated that the hard phase (H) had an approximate composition (wt. %) of 74% Pd, 11% Cu and 10% Ga, along with 1-2% Sn, Au and Ru. The surrounding grain boundary phase (G) had a similar composition, except for a lower copper content (8%). There were minimal changes in the microstructure after heat treatment at temperatures from 200° to 800°F. A small increase in the amount of the hard phase, compared to that in the ACRQ condition, which was observed after heat treatment at 1,000°F, might have contributed to the highest mean hardness (Table 3). After the heat treatments at 1,200° and 1,400°F, discontinuous precipitates with a lamellar morphology (Shewmon, 1969) were observed near grain boundaries (Fig. 5). This figure shows that at higher magnification, the hard phase (H) typically appeared as narrow parallel bands in contact, perhaps due to extensive twinning or slip which would contribute to hardness.

The composition of the hard phase (H) approximately matches Pd_5Ga_2, and the surrounding grain boundary phase (G) is assumed to be Pd_2Ga. Both phases can have a relatively wide variation in the Pd/Ga ratio at elevated temperatures (Fig. 1); this suggests that substantial solid solution incorporation of other elements is also possible. Further examination of the Pd-Ga phase diagram (Fig. 1) also suggests that the discontinuous precipitates (Fig. 5) are alternating lamellae of $Pd_{13}Ga_5$ and the palladium solid solution. (Discontinuous precipitates in the other three alloys are also assumed to consist of these two phases, which contain small amounts of other elements from the alloy composition in substitutional solid solution.) However, planned X-ray diffraction studies of model alloys are necessary for unambiguous phase identification. The extensive solute diffusion and redistribution required for formation of the discontinuous precipitates is facilitated by the submicron thickness of the lamellae.

When the heat-treatment temperature was increased above 1,600°F, the discontinuous precipitates began to dissolve into the palladium solid solution. After heat treatment at 1,800°F, both the eutectic constituent and the discontinuous precipitates were no longer present (Fig. 6), and the hard phase morphology of Figure 4 had largely disappeared. A remaining grain boundary phase in the form of widely separated, globular particles had a similar composition and hardness as the surrounding grain boundary phase (G), suggesting that this phase was

Figures 9-14 on the facing page 169

Figure 9. Secondary electron image of ACBC Pd-Ga alloy Legacy XT, showing the embedded Ru-rich precipitates (R), as well as two types of grain boundary precipitates (P1 and P2). Bar = 10 μm.

Figure 10. Secondary electron image of ACBC Legacy XT, showing an embedded Ru-rich precipitate with a dramatic morphology. Bar = 10 μm.

Figure 11. Secondary electron image of Legacy XT after heat treatment at 1,200°F, showing the formation of lamellar discontinuous precipitates (D) and larger island-shaped precipitates (P). Bar = 10 μm.

Figure 12. Secondary electron image of ACBC Pd-Ga alloy IS 85, showing the dendritic structure. Bar = 100 μm.

Figure 13. Secondary electron image of IS 85 after heat treatment at 1,200°F, showing the formation of discontinuous precipitates. Bar = 10 μm.

Figure 14. Secondary electron image of IS 85 after heat treatment at 1,800°F, showing the disappearance of the discontinuous precipitates. The persistence of a dendritic structure and a network of hot tears can be seen. Bar = 100 μm.

----

also Pd_2Ga. The presence of the palladium solid solution and Pd_2Ga is consistent with the Pd-Ga phase diagram at 1,800°F. A surface oxidation band about 30 μm thick was also observed after heat treatment at 1,800°F (Wu, 1996). Recent X-ray diffraction analyses (Brantley *et al.*, 1996a) of Liberty following oxidation of a polished and etched surface indicated that the major oxides were SnO_2, $CuGa_2O_4$ and Cu_2O; β-Ga_2O_3 and PdO·xH_2O also appeared to be present in the complex layer.

The significant decrease in the hardness of Liberty as the heat-treatment temperature was increased from 1,200° to 1,800°F (Table 3) was attributed to an observed decrease in the amount of the hard phase (H). Measurements with a 10 g load indicated that the values of hardness for the eutectic structure and the discontinuous precipitates were nearly identical to that for the palladium solid solution matrix in Liberty. Consequently, these fine-scale lamellar constituents provide no additional strengthening for this alloy.

The other Pd-Cu-Ga alloy, Freedom Plus, had a fine-grained microstructure that also contained a residual dendritic structure which was particularly evident at low magnification. The complex microstructure of ACBC Freedom Plus in Figure 7 contains residual interdendritic
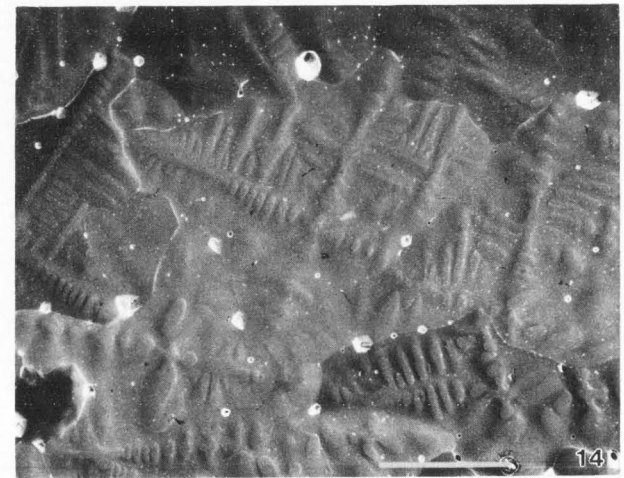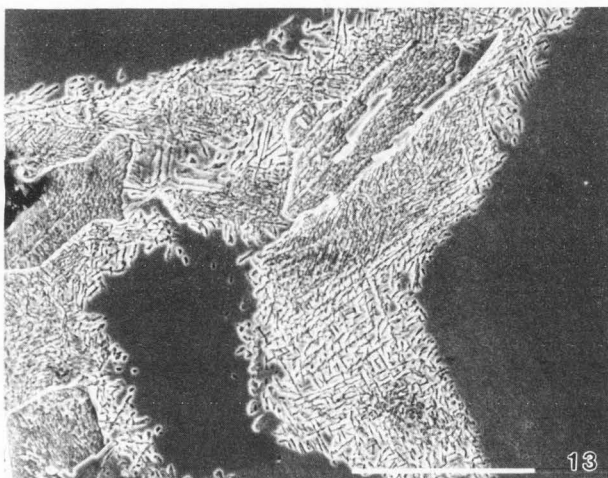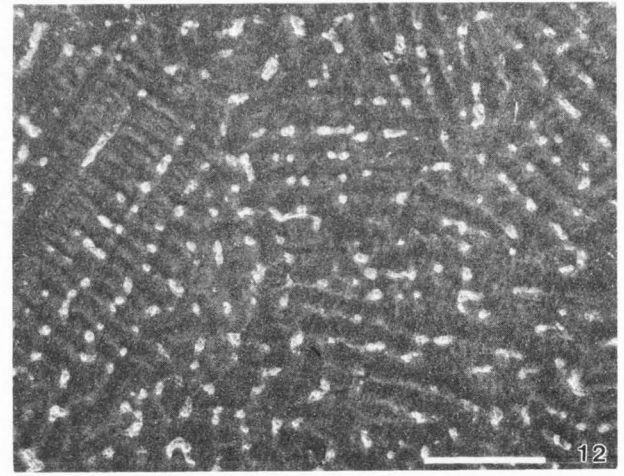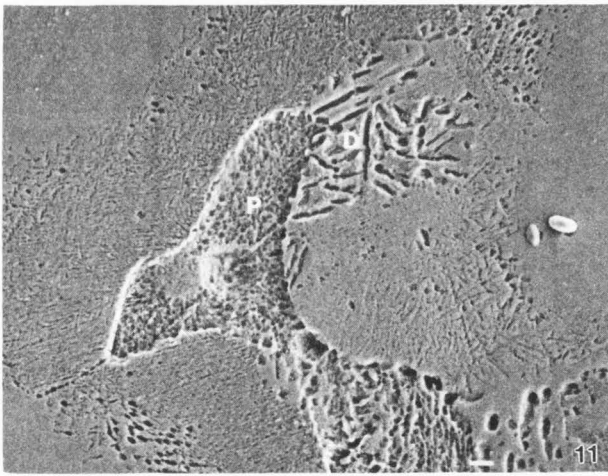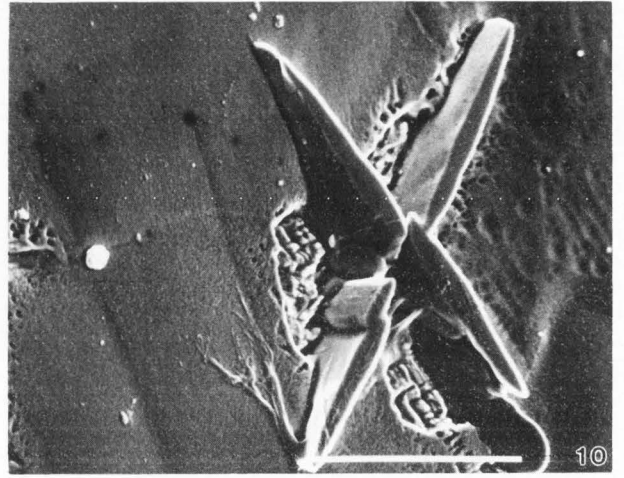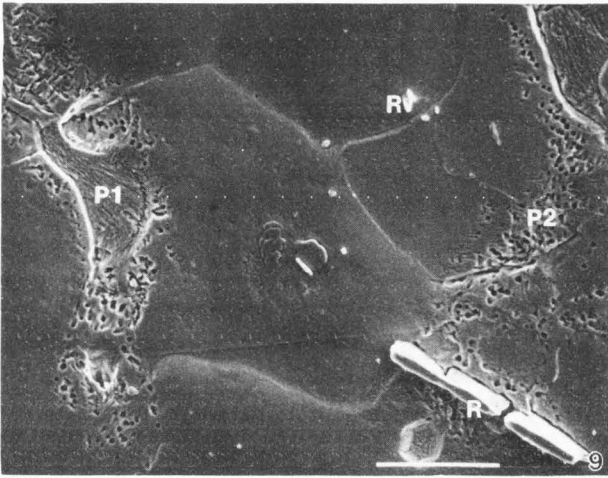
Table 4. Approximate phase transformation temperatures (°F) of the four high-palladium alloys determined from TMA experiments.[*]

Alloy ------>	Liberty	Freedom Plus	Legacy XT	IS 85
Transformation Temperature (Heating cycle)	$1,417 \pm 51$	$1,357 \pm 52$	$1,413 \pm 38$	$1,425 \pm 45$
Transformation Temperature (Cooling cycle)	$1,087 \pm 24$	$1,047 \pm 27$	$1,049 \pm 18$	$1,049 \pm 24$

[*]N = 5 for each alloy other than Legacy XT (N = 4).

---

regions (I), a grain boundary eutectic structure (E), a relatively wide grain boundary phase (G) with hardness very similar to that for the surrounding grain boundary phase (G) in Figure 4, and white-appearing Ru-rich precipitates (R) that have been previously discussed (Brantley *et al.*, 1993). The microstructure of ACRQ Freedom Plus contained less grain boundary eutectic structure, a greater width for the wide grain boundary phase (particularly in the near-surface region) and less Ru-rich precipitates. The higher melting range (Table 2) and lower prevalence of the eutectic microstructural constituent for Freedom Plus compared to Liberty suggests that the composition of Freedom Plus is closer to the limit of the range where a eutectic constituent forms in the solidifying alloy.

Heat treatments at temperatures from 200° to 1,000°F caused little change in the microstructure of Freedom Plus. Discontinuous precipitates, which were no harder than the palladium solid solution, appeared at the grain boundaries after heat treatments at 1,200° (Fig. 8) and 1,400°F. There was some disappearance of the discontinuous precipitates after heat treatment at 1,600°F, and they were no longer present after heat treatment at 1,800°F, where the microstructure consisted only of the palladium solid solution and some Ru-rich precipitates (Wu, 1996). Because Freedom Plus contained much smaller amounts of the hard phase found in Liberty, the hardness was nearly independent of solidification condition and heat-treatment temperature (Table 3).

The fine-grained microstructure of the Pd-Ga alloy Legacy XT in the ACBC condition contained large embedded precipitates, identified by EDS as Ru-rich, and two different types of grain-boundary precipitates (Fig. 9); there was little difference in the microstructure for the ACRQ condition. Some of the Ru-rich precipitates in this alloy had a striking morphology (Fig. 10). It is conjectured that many Ru-rich seed crystallites for grain refinement (Brantley *et al.*, 1993) were too small for observation with the SEM. The first type of grain-boundary precipitate (P1) consisted of isolated particles with dimensions of 5-10 μm, whereas the second type (P2) consisted of numerous particles less than 0.5 μm in dimensions. Because of the high contents of silver (10 wt. %) and indium (6 wt. %) in Legacy XT (Table 1), consideration of the binary diagrams (Massalski, 1986; Brantley *et al.*, 1993) suggests that Ag-In phases may form in this alloy, and Pd-Ga, Pd-In and Ga-In phases are also possible, particularly if microsegregation alters the local ratio of the elemental components.

Heat treatment of Legacy XT at temperatures between 200° and 1,000°F resulted in minimal microstructural changes. Heat treatment at 1,200°F caused the formation of numerous discontinuous precipitates, which again had a very similar hardness to that of the palladium solid solution, along with another type of relatively large precipitate (Fig. 11). While there was little microstructural change after heat treatment at 1,400°F, the discontinuous precipitates began to disappear after heat treatment at 1,600°F, and only the palladium solid solution and Ru-rich precipitates remained after heat treatment at 1,800°F (Wu, 1996). The absence of a hard microstructural phase similar to that found in Liberty is considered to account for the minor dependence of the hardness of Legacy XT on solidification condition and heat-treatment temperature (Table 3).

The dendritic structure of the Pd-Ga alloy IS 85 in the ACBC condition is shown in Figure 12, where several colonies of dendrites with different orientations are evident. The width of the dendrites and the size of the interdendritic regions (bright areas in Fig. 12, confirmed by observations at higher magnifications) were smaller for the ACRQ condition because the higher rate of solidification allowed less time for growth. When examined at the same magnification (Wu, 1996), the complex interdendritic regions in IS 85 contained constituents that resembled the grain boundary precipitates in ACBC Freedom Plus (Fig. 7) and the grain boundary precipitates in ACBC Legacy XT (Fig. 9).

There was minimal change in the dendritic micro-

structure of IS 85 until the heat-treatment temperature reached 1,200°F, where a substantial amount of discontinuous precipitates formed at the sites of the former interdendritic regions (Fig. 13). The discontinuous precipitates began to disappear with heat treatment at 1,600°F (Wu, 1996) and were no longer present after heat treatment at 1,800°F (Fig. 14). There was some persistence of the original dendritic structure, unlike the effect of heat treatment at 1,800°F on the 79Pd-10Cu-9Ga-2Au alloys, Spartan, Spartan Plus (Williams/Ivoclar) and Option (Brantley et al., 1996c). The type of microstructure in Figure 14 has been termed a **dendrite grain structure** (Skolianos et al., 1983).

There was still evidence of the dendritic structure even after IS 85 was subjected to the complete firing cycles (Papazoglou et al., 1993) for a dental porcelain. Previously, it was found that this more extensive heat treatment eliminated the as-cast dendritic structure in Spartan (Brantley et al., 1993; Carr et al., 1993), and the same heat-treatment response is expected for Option and Spartan Plus (Brantley et al., 1996c). It is presumed that the diffusion rates for one or more of the elements tin, indium and silver in IS 85 (Table 1), which were not present in the three 79Pd-10Cu-9Ga-2Au alloys, were too low for microstructural homogenization during the simulated porcelain-firing heat treatment.

In the present study, IS 85 was the only alloy that exhibited hot tears (Fig. 14), i.e., microscopic cracks that are a consequence of the dendritic structure (Carr et al., 1993). The hot tears were observed near the specimen surface and occur because the interdendritic regions, which undergo solidification last, may not have sufficient strength to withstand the stresses imposed by the palladium solid solution dendrites and the investment during cooling of the casting. The hot tears are expected to occur in thin sections of castings where the cooling rate is greater and there is inadequate metal support. These microstructural defects are potential sources of crack propagation that may result in failure of the casting under *in vivo* loading. These microscopic fractures were previously observed in dendritic Pd-Cu-Ga alloys (Carr et al., 1993; Brantley et al., 1996c). Since IS 85 was designed for implant-supported prosthetic applications (Stewart et al., 1992), castings of this alloy should normally have a thickness that is adequate to minimize the occurrence of hot tears.

Thermomechanical analysis (TMA) experiments

Figure 15 is a TMA plot of the dimensional changes for a Liberty specimen between room temperature and 1,800°F, at heating and cooling rates of 9°F per minute. For each alloy, the TMA plots for all five specimens were very similar. Each heating and cooling curve consisted of two relatively straight segments of constant
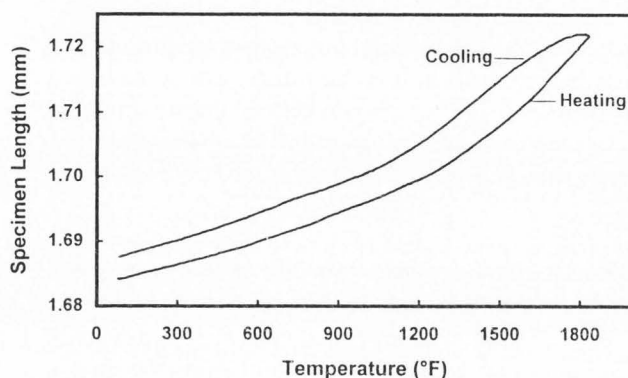

Figure 15. Heating and cooling thermomechanical analysis (TMA) curves for the Liberty alloy.

---

slope (linear coefficient of thermal expansion, α) separated by a transition region. Extrapolation of these linear segments, as shown in Figure 15, yields a point of inflection that is conventionally set as the phase transformation temperature (Wendlandt, 1986), even though the transformation takes place over a range of temperatures. Using this procedure, the phase transformation temperature of the high-palladium alloys during heating ranged from 1,357° to 1,425°F, while the transformation temperature on cooling ranged from 1,047° to 1,087°F (Table 4). Because of the somewhat irregular appearance of the TMA plot for one Legacy XT specimen, the means and standard deviations for this alloy are based upon four rather than five specimens as for the other three alloys.

Figure 15 shows that the high-palladium alloys undergo second-order phase transformations on heating and cooling, where the specimen length (l) is continuous with temperature but the rate of change in specimen length with temperature ($dl/dT = \alpha$) is discontinuous (Rosen, 1993). The hysteresis between the heating and cooling transformation temperatures (Table 4) is due to the dynamic nature of the TMA experiments. Additional thermal energy must be supplied to initiate the heating transformation, and subsequently removed to initiate the cooling transformation, compared to equilibrium conditions. Consequently, the transformation temperature for the TMA heating cycle exceeds the equilibrium transformation temperature while the transformation temperature for the cooling cycle is less than the equilibrium transformation temperature. Recent transmission electron microscopy studies have shown that a submicron ordered tweed structure is present in the ultrastructures of several representative high-palladium dental alloys for both the as-cast and heat-treated conditions (Cai, 1996). This tweed structure has a very similar appearance to the submicron precipitate network in a Pd-Cu-Ga alloy that was previously reported by Odén and Herø (1986). Since

discontinuous precipitation is a first-order transformation and ordering can be a second-order phase transformation where there is compositional uniformity across the interface (Christian, 1975), it is conjectured that an ordering reaction accounts for the present TMA observations.

Conclusions

Based on the results of this investigation, the following conclusions can be drawn:

(1). Of the four high-palladium dental alloys studied in the as-cast condition, only the Liberty Pd-Cu-Ga alloy had a clinically significant response to heat treatment, which occurred only for heat-treatment temperatures of 1,600° and 1,800°F. The Freedom Plus Pd-Cu-Ga alloy and the Legacy XT and IS 85 Pd-Ga alloys were relatively unresponsive to heat treatment over the temperature range from 200° to 1,800°F. Measurements of Vickers hardness, which should correlate with alloy yield strength, were used to judge the responsiveness to heat treatment.

(2). The higher hardness of Liberty was due to a previously unidentified, hard phase (Vickers hardness exceeding 400) having an approximate composition (wt.%) of 74% Pd, 11% Cu and 10% Ga, along with minor amounts of Sn, Au and Ru. This hard phase, assumed to be Pd_5Ga_2, appeared to be present in small amounts in the microstructure of Freedom Plus, and was absent in the microstructures of Legacy XT and IS 85. The eutectic constituent in Liberty was found to have nearly the same hardness as the palladium solid solution.

(3). Discontinuous precipitates formed in all four high-palladium alloys during heat treatment at 1,200° to 1,400°F. While these fine-scale lamellar phases are assumed to consist of the palladium solid solution and $Pd_{13}Ga_5$ resulting from decomposition of the supersaturated palladium solid solution, X-ray diffraction is required to confirm this hypothesis. The discontinuous precipitates always had the same hardness as the palladium solid solution in each alloy. These precipitates were not present in the four alloys after heat treatment at 1,800°F, which yielded a microstructure containing only the palladium solid solution and ruthenium-rich precipitates for Freedom Plus and Legacy XT, and a microstructure containing the palladium solid solution, a Pd_2Ga grain boundary phase and ruthenium-rich precipitates for Liberty.

(4). The IS 85 alloy, which did not contain the grain-refining element ruthenium, had a dendritic microstructure that persisted after heat treatment at 1,800°F. The residual dendrite structure is attributed to the relatively slow diffusion rates of one or more of the elements tin, indium and silver, which did not permit microstructural homogenization during heat treatment.

(5). The TMA experiments indicated that all four high-palladium alloys underwent a second-order phase transformation that may be associated with the formation of an ordered tweed structure observed by transmission electron microscopy in another study.

Acknowledgment

References

Asgar K (1988) Casting metals in dentistry: Past-present-future. Adv Dent Res **2**, 33-43.

Bertolotti RL (1997) Alloys for porcelain-fused-to-metal restorations. In: Dental Materials: Properties and Selection (2nd ed). O'Brien WJ (ed.). Quintessence, Chicago. Chap 16.

Brantley WA, Cai Z, Carr AB, Mitchell JC (1993) Metallurgical structures of as-cast and heat-treated high-palladium dental alloys. Cells Mater **3**, 103-114.

Brantley WA, Cai Z, Foreman DW, Mitchell JC, Papazoglou E, Carr AB (1995) X-ray diffraction studies of as-cast high-palladium alloys. Dent Mater **11**, 154-160.

Brantley WA, Cai Z, Papazoglou E, Mitchell JC, Kerber SJ, Mann GP, Barr TL (1996a) X-ray diffraction studies of oxidized high-palladium alloys. Dent Mater **12**, 333-341.

Brantley WA, Cai Z, Vermilyea SG, Papazoglou E, Mitchell JC, Carr AB (1996b) Effects of solidification conditions and heat treatment on the microstructures and Vickers hardness of Pd-Cu-Ga dental alloys. Cells Mater **6**, 127-135.

Brantley WA, Wu Q, Cai Z, Vermilyea SG, Mitchell JC (1996c) Effects of casting conditions and annealing on dendritic Pd-Cu-Ga alloys. J Dent Res **75**, 60 (IADR Abst. no. 339).

Cai Z (1996) Metallurgical Structures, *In Vitro* Corrosion Resistance and Biocompatibility of High-Palladium Dental Casting Alloys. PhD Dissertation, The Ohio State University, Columbus, OH.

Carr AB, Brantley WA (1991) New high-palladium casting alloys: Part 1. Overview and initial studies. Int J Prosthodont **4**, 265-275.

Carr AB, Cai Z, Brantley WA, Mitchell JC (1993) New high-palladium casting alloys: Part 2. Effects of heat treatment and burnout temperature. Int J Prosthodont **6**, 233-241.

Cascone PJ (1984) Phase relations of the palladium-base, copper, gallium, indium alloy system. J Dent Res

63, 233 (IADR Abst. no. 563).

Christian JW (1975) The Theory of Transformations in Metals and Alloys (2nd ed.). Pergamon Press, Oxford (U.K.). pp. 206-226 and 504-523.

Craig RG (ed.) (1993) Restorative Dental Materials (9th ed.). Mosby, St Louis, MO. pp. 86-90.

Darken LS, Gurry RW (1953) Physical Chemistry of Metals. McGraw-Hill, New York. pp. 283-294.

Dieter GE (1986) Mechanical Metallurgy (3rd ed.). McGraw-Hill, New York. pp. 329-332.

Khabliyev SZ-B, Sakhanskaya IN, Cheremnykh VG, Litvinov VS (1980) Phase transformations in a high-duty alloy of palladium with copper and gallium. Phys Met Metall 47, 187-189.

Khalaff K, Schubert K (1974) Kristallstruktur von Pd_5Ga_2 (Crystal structure of Pd_5Ga_2). J Less-Common Metals 37, 129-140.

Massalski TB (editor-in-chief) (1986) Binary Alloy Phase Diagrams. Vols. 1 and 2. American Society for Metals, Metals Park, OH. pp. 34, 1136, 1153 and 1390.

Massalski TB (editor-in-chief) (1990) Binary Alloy Phase Diagrams (2nd ed.), Vol. 2. ASM International, Materials Park, OH. pp. 1836 and 1838.

Mezger PR, Stols ALH, Vrijhoef MMA, Greener EH (1988) Metallurgical aspects of high-palladium alloys. J Dent Res 67, 1307-1311.

Odén A, Herø H (1986) The relationship between hardness and structure of Pd-Cu-Ga alloys. J Dent Res 65, 75-79.

Papazoglou E, Brantley WA, Carr AB, Johnston WM (1993) Porcelain adherence to high-palladium alloys. J Prosthet Dent 70, 386-394.

Phillips RW (1991) Skinner's Science of Dental Materials (9th ed.). Saunders, Philadelphia. pp. 427-430.

Reed-Hill RE, Abbaschian R (1994) Physical Metallurgy Principles (3rd ed.). PWS Publishing, Boston. pp. 336-340 and 461-466.

Rosen SL (1993) Fundamental Principles of Polymeric Materials (2nd ed.). Wiley, New York. pp. 104-106.

Schaffer SP (1983). Novel palladium alloy and dental restorations utilizing same. US Patent 4,387,072.

Schubert K, Lukas HL, Meissner H-G, Bhan S (1959) Zum aufbau der systeme kobalt-gallium, palladium-gallium, palladium-zinn und verwandter legierungen (On phases in the systems cobalt-gallium, palladium-gallium, palladium-tin and related alloys). Z Metallkde 50, 534-540.

Skolianos S, Liu P-S, Kattamis TZ (1983) Effect of coarsening during solidification on the microstructure of Al and Mg alloys. In: Grain Refinement in Castings and Welds. Abbaschian GJ, David SA (eds.). American Institute of Mining, Metallurgical and Petroleum Engineers (AIME), Warrendale, PA. pp. 94-115.

Shewmon PG (1969) Transformations in Metals. McGraw-Hill, New York. pp. 267-274.

Stewart RB, Gretz K, Brantley WA (1992) A new high-palladium alloy for implant-supported prostheses. J Dent Res 71, 158 (AADR Abst. no. 423).

van der Zel JM (1989) High-Temperature Behavior of Palladium-Based Dental Alloys. Doctoral Thesis, University of Amsterdam, The Netherlands.

Wendlandt WW (1986) Thermal Analysis (3rd ed.). Wiley, New York. pp. 686-692.

Wu Q (1996) Heat Treatment Behavior for High-Palladium Dental Alloys. MS Thesis, The Ohio State University, Columbus, OH.

Discussion with Reviewers

H.J. Mueller: While results from this study have demonstrated that heat treatment-property relationships are limited for commercially available high-palladium dental alloys, should future alloy development strive to design compositions amenable to heat treatment, so that properties useful for clinical applications can be varied over a wider range?

Authors: Our research has indicated that the Pd-Cu-Ga alloys, such as Liberty, that contain relatively higher amounts of Cu and Ga, and form the hard phase (H), are the most responsive to such heat treatment. Studies are presently underway in our laboratory to determine whether the values of Vickers hardness for representative high-palladium alloys correlate with yield strength, as expected from principles of mechanical metallurgy (Dieter, 1986). However, we have noted that there is some concern about the biocompatibility of Pd-Cu-Ga alloys that have lamellar eutectic microstructural constituents (Cai *et al.*, 1995).

H.J. Mueller: Is there any benefit for retaining a dendritic microstructure, such as that shown in Figure 14? Should the differences in percentage elongation and yield strength for the alloys presented in Table 2 be attributed to microstructural or compositional effects?

Authors: Because of the potential for forming "hot tears" in the microstructure during cooling (Carr *et al.*, 1993), some caution should be exercised about the selection of high-palladium alloys that have dendritic as-cast microstructures where there is insufficient supporting metal, such as in thin marginal areas of castings. For the alloys in Table 2, the differences in yield strength and percentage elongation appear to arise from variations in microstructures that are closely linked to the alloy compositions.

M.D. Bagby: Is the proposed mechanism for hot tearing related to the absence of grain refiners?

Authors: Yes. The high-palladium dental alloys that contain sufficient amounts of ruthenium as a grain-refining element form equiaxed fine-grained microstructures (Brantley *et al.*, 1993). We have only observed hot tears in high-palladium alloys with dendritic microstructures, where the weaker interdendritic regions provide facile paths for crack propagation as the investment imposes stresses on the cooling alloy after solidification (Carr *et al.*, 1993). The principal factors for the formation of hot tears are investment mold temperature, cooling rate during solidification (bench cooled or quenched) and thickness of supporting metal in the casting.

M.D. Bagby: Does this work support the proposition that Ga diffuses faster in high-palladium alloys and therefore might be better at forming an oxide layer for porcelain bonding, as compared to Sn and In?
Authors: We are unable to draw this conclusion from the present study. We are currently comparing the roles of these elements in forming oxide layers on Pd-Ga alloys and contributing to porcelain adherence (Papazoglou *et al.*, 1997).

R.A. Fournelle: Where did the discontinuous precipitates form in the Liberty alloy: in the region containing the large amount of eutectic or well in the interior where there appeared to be little eutectic?
Authors: The discontinuous precipitates appeared to form around grain boundaries in both the surface and bulk regions. Since the appearances of the discontinuous precipitates and the eutectic are very similar, it is difficult to distinguish between the two constituents.

R.A. Fournelle: Could the narrow bands in the hard phase (H) in Figure 5 also be due to a martensitic phase transformation occurring on cooling to room temperature? How else would one get slip and twinning to occur if not by a shear-type phase transformation?
Authors: A martensitic phase transformation may be occurring. In his recent transmission electron microscopy study of high-palladium dental alloys, Cai (1996) concluded that the submicron ordered tweed structure formed by a martensitic transformation. At the much coarser microstructural scale in Figures 4 and 5, we considered that differences in the thermal contraction when the G and H phases formed during solidification might create sufficient local stress to cause slip or twinning. Since the Pd_5Ga_2 phase might have relatively few active slip systems, we considered that twinning of the H phase would be plausible.

O. Johari: Since the international scientific community commonly uses the Celsius temperature scale, why have

Table 5. Temperatures in °F and °C.

Temperature (°F)	Temperature (°C)[*]
200	90
400	200
600	320
800	430
1000	540
1200	650
1400	760
1600	870
1800	980

[*]Rounded to nearest ten degrees.

----

the authors used the Fahrenheit temperature scale throughout their article?
Authors: We have adopted this style, which is common in the dental literature, because the dental laboratory furnaces, the instructions from dental manufacturers for the heating of dental casting investment and the firing cycles for dental porcelain use the Fahrenheit temperature scale. Because the reprinted Pd-Ga phase diagram in Figure 1 uses the Celsius scale, we are providing a conversion table (Table 5) to facilitate comparisons of the heat-treatment temperatures to important phase fields.

Additional References

Cai Z, Chu X, Bradway SD, Papazoglou E, Brantley WA (1995) On the biocompatibility of high-palladium dental alloys. Cells Mater **5**, 357-368.

Papazoglou E, Brantley WA, Mitchell JC (1997) Porcelain adherence and oxidation of Pd-Ga alloys. J Dent Res **76**, 402 (IADR Abst. no. 3108).